Preparation and properties of sulfonated poly(fluorenyl ether ketone) membrane for vanadium redox flow battery application

Dongyang Chen, Shuanjin Wang*, Min Xiao, Yuezhong Meng**

State Key Laboratory of Optoelectronic Materials and Technologies/The Key Laboratory of Low-carbon Chemistry & Energy Conservation of Guangdong Province, Sun Yat-Sen University, Guangzhou 510275, PR China
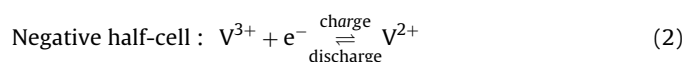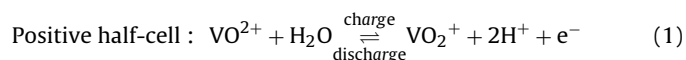
ARTICLE INFO

ABSTRACT

In order to develop novel membranes for vanadium redox flow battery (VRB) with low self-discharge rate and low cost, sulfonated poly(fluorenyl ether ketone) (SPFEK) was synthesized directly via aromatic nucleophilic polycondensation of bisphenol fluorene with 60% sulfonated difluorobenzophenone and 40% difluorobenzophenone. The SPFEK membrane shows the lower permeability of vanadium ions. The open circuit voltage evaluation demonstrates that the SPFEK membrane is superior to Nafion 117 membrane in self-discharge test. Both energy efficiencies (EE) and power densities of the VRB single cell based on the SPFEK membrane are higher than those of the VRB with Nafion 117 membrane at the same current densities. The highest coulombic efficiency (CE) of VRB with SPFEK membrane is 80.3% while the highest CE of the VRB with Nafion 117 membrane is 77.0%. The SPFEK membrane shows the comparative stability to Nafion 117 membrane in VO_2^+ electrolyte. The experimental results suggest that SPFEK membrane is a promising ion exchange membrane for VRB.

© 2009 Elsevier B.V. All rights reserved.
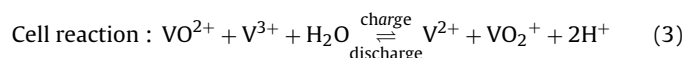
1. Introduction

Vanadium redox flow battery (VRB) has been attracting more and more attentions since it was first proposed by Skyllas-Kazacos and his co-workers [1]. It is a promising electrochemical energy storage battery for its high power density, various loading levels and considerable energy efficiency. It employs V^{2+}/V^{3+} and VO_2^+/VO^{2+} redox couples in sulfuric acid solution as its negative and positive half-cell electrolytes and an ion exchange membrane as its separator. Electrolytes stored in two tanks were pumped and circulated through the stack where electrochemical reaction occurred. In the charge and discharge processes, the following reaction happened:

$$\text{Positive half-cell}: \ VO^{2+} + H_2O \underset{\text{discharge}}{\overset{\text{charge}}{\rightleftharpoons}} VO_2^+ + 2H^+ + e^- \qquad (1)$$

$$\text{Negative half-cell}: \ V^{3+} + e^- \underset{\text{discharge}}{\overset{\text{charge}}{\rightleftharpoons}} V^{2+} \qquad (2)$$

$$\text{Cell reaction}: \ VO^{2+} + V^{3+} + H_2O \underset{\text{discharge}}{\overset{\text{charge}}{\rightleftharpoons}} V^{2+} + VO_2^+ + 2H^+ \qquad (3)$$

From the above reaction we can reach that only ions of vanadium are involved in the redox processes, which eliminated cross-contamination between the two electrolyte tanks. Furthermore, there is production and consumption of proton on the electrode, which make proton to be an effective charge carrier to transport through the separator completing the circuit during the passage of current. Since the electrolytes are flowing unceasingly, the concentration polarization can be reduced and the mass loss of active species can be avoided.

Recently, many works have been carried out on the development of suitable and stable membrane for the battery application [2–8]. Most of them were focused on the modification of commercialized cationic exchange membranes as well as anionic exchange membranes. Using anionic exchange membrane will effectively reduce the permeation of vanadium ions through the membrane owning to Donnan exclusion effect, but it will not assist the conduction of proton which results in the sacrifice of voltage efficiency of the battery. Using cationic exchange membrane is difficult to prevent the permeation of vanadium ions with passage of protons; however, it guarantees lower resistance of the membrane and the possibility of higher energy efficiency. Nafion membrane (DuPont) is the most commonly used proton conducting membrane for its high proton conductivity and excellent chemical stability. So, many attempts were made to use it or its hybrid membranes as VRB separator [9]. It is demonstrated in the literatures as well as in this paper

---

* Corresponding author.
** Corresponding author at: School of Physics & Engineering, State Key Laboratory of Optoelectronic Materials and Technologies/The Key Laboratory of Low-carbon Chemistry & Energy Conservation of Guangdong Province, Sun Yat-Sen University, Guangzhou, Guangdong 510275, PR China. Tel.: +86 20 84114113; fax: +86 20 84114113.
E-mail addresses: wangshj@mail.sysu.edu.cn (S. Wang),
mengyzh@mail.sysu.edu.cn (Y. Meng).

that Nafion membrane suffers from the undesirable crossover of vanadium ions during the charge–discharge processes of VRB for its low permeation selectivity between proton and vanadium ions.

A number of aromatic polymers such as poly(phthalazinone ether)s [10], poly(arylene ether ketone)s [11–13], polyimides [14], poly(arylene sulfone)s [15,16]. were functionalized to give proton conductive ability by introducing carboxylic acid group, phosphonic acid group or sulfonic acid group onto the backbone or onto the pendant chains of the parent polymer. Presently, there are few reports on using sulfonated aromatic polyethers as separators of all vanadium redox flow battery. We have reported a novel sulfonated poly(fluorenyl ether ketone) (SPFEK) with high proton conductivity in the previous paper [17]. In our laboratory, we have scaled up the synthesis of the sulfonated poly(fluorenyl ether ketone) and the preparation of membrane. Herein, we will explore the application of the SPFEK membrane in the VRBs. The properties of the SPFEK membrane for VRBs were investigated and compared with Nafion 117 membrane. The VRB cell performance was also investigated in detail in order to develop an appropriate membrane for all vanadium redox flow battery.

2. Experimental

2.1. Preparation of sulfonated poly(fluorenyl ether ketone) membrane

The SPFEK polymer used was obtained from the scale up production line of our laboratory, and the synthesis procedure has been published earlier [17]. The structure of SPFEK is depicted in Scheme 1.

The SPFEK membranes were prepared by casting a viscous solution in N,N′-dimethylacetamide (DMAc) onto a glass plate in a dust-free environment. The thickness of membrane was controlled by the amount and the concentration of the polymer solution. Membranes were dried at 60 °C for 12 h and then at 110 °C under vacuum for 48 h. Sodium-form membranes were transformed into proton-form membrane by soaking in hot 0.5 M H_2SO_4 aqueous solution for 2 h and in distilled water for 2 h. They were stored in distilled water until used.

2.2. Membrane characterization

Proton conductivity of the membrane was determined by electrochemical impedance spectroscopy. The impedance of a membrane was measured in a cell with the given membrane sample sandwiched between two gold electrodes. The measurements were carried out on a Solartron 1255 B frequency response analyzer coupled with a Solartron 1287 electrochemical interface in the frequency range of 1 Hz to 1 MHz at 25 °C. The conductivity was calculated from the impedance plot with a computer curve-fitting technique according to the electrode area of the cell and the thickness of the membrane, which was measured with a micrometer.

The proton conductivity (σ) of the specimen in the transverse direction (across the membrane) was calculated from the impedance data according the following equation (Eq. (4)):

$$\sigma \ (s/cm) = \frac{d}{RS} \tag{4}$$

where d and S are the thickness and the face area of the specimen, respectively, and R is derived from the low intersect of the high frequency semicircle on a complex impedance plane with the Re (Z') axis.

The water uptake of the membranes was defined as weight ratio of the absorbed water to that of the dry membrane. The swelling ratio was described as the linear expansion rate of wet membrane.

They can be calculated via the following Eqs. (5) and (6):

$$W \ (\%) = \frac{(W_w - W_d)}{W_d} \times 100\% \tag{5}$$

$$L \ (\%) = \frac{L_1 - L_0}{L_0} \times 100\% \tag{6}$$

where W_d and W_w are the weight of membranes before and after water absorption, respectively; L_0 and L_1 are the length of membranes before and after water absorption, respectively.

Ion exchange capacity (IEC) was measured by titration. The dried membrane was weighed and immersed in 1 M HCl solution for 5 h to give the membrane in H-form and then washed with excess amount of deionized water until PH was neutral. The membrane was then immersed in 2 M NaCl solution and the replaced proton was titrated using 0.1 M NaOH solution with phenolphthalein as indicator. IEC was calculated by following Eqs. (7):

$$IEC = \frac{\Delta V_{NaOH} C_{NaOH}}{W_d} \tag{7}$$

where W_d is the weight of the dry membrane, ΔV_{NaOH} is the consumed volume of NaOH solution and C_{NaOH} is the concentration of NaOH solution.

Tensile strength was determined at 25 °C and 50% relative humidity by a universal test machine (Model CMT-4014 SANS, Shenzhen, China). The cross-head speed was set at a constant speed of 10 mm min^{-1}. The samples were cut into a size of 5 mm × 50 mm. For each material tested, at least three measurements were taken and average value was calculated.

The permeability of VO^{2+} was measured by the method according to the literature [18]. 40 mL of 1 M $VOSO_4$ in 2 M H_2SO_4 solution was filled in one reservoir and 40 mL of 1 M $MgSO_4$ in 2 M H_2SO_4 solution was filled in the other reservoir. The two reservoirs were separated by the membrane samples. $MgSO_4$ was used to equalize the osmotic pressure. The two solutions were continuously magnetic stirred at different temperatures. Samples of the $MgSO_4$ solution were taken at a regular time interval and the concentration of VO^{2+} was measured by UV–vis spectrophotometer (Model: 752-P, Shanghai Xianke CO. China) for each temperature. The membrane area exposed to electrolytes was 5.3 cm^2.

2.3. Cell tests

Charge–discharge test was carried out by sandwiching the membrane between two pieces of carbon felts (Shanghai Morgan Carbon Co., Ltd., China), which was served as the electrodes and the graphite plates with serpentine flow fields were served as the current collectors. The electrolytes used were 40 mL of 1 M VO^{2+} in 2 M H_2SO_4 solution as anodic electrolyte and 40 mL of 1 M V^{3+} in 2 M H_2SO_4 solution as cathodic electrolyte. They were pumped through the cell unceasingly during the test at room temperature. The schematic apparatus setup is depicted in Fig. 1. The effective area of membrane was 4.86 cm^2 while the end voltage for discharging was set to 0.7 V. Experimental data were recorded on Solartron electrochemical interface 1287 using galvanostatic and potentialstatic technologies. The coulombic efficiency (CE) and energy efficiency (EE) of the cell were calculated by following Eqs. (8) and (9):

$$CE = \frac{C_d}{C_{tc}} \times 100\% \tag{8}$$

$$EE = \frac{E_d}{E_{tc}} \times 100\% \tag{9}$$

where C_d is the discharge capacity and C_{tc} is the theoretic charge capacity of the cell. C_{tc} is based on the amount of the active materials using Faraday's equation. E_d is referred to the discharged electric energy of the cell. E_{tc} is referred to the theoretic charged electric
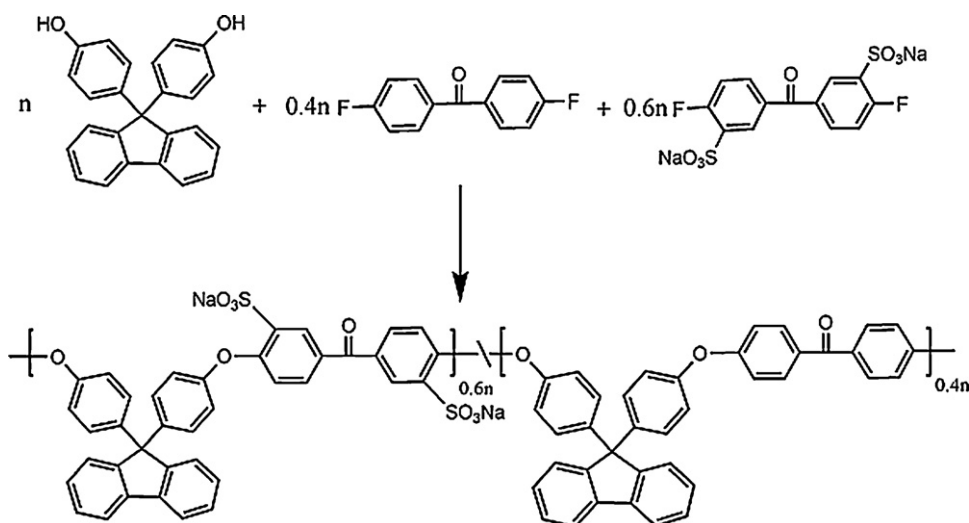
Scheme 1. Synthesis of sulfonated poly(fluorenyl ether ketone). The backslash in the resulting copolymer structure means the copolymer is a random copolymer of the separated segments.
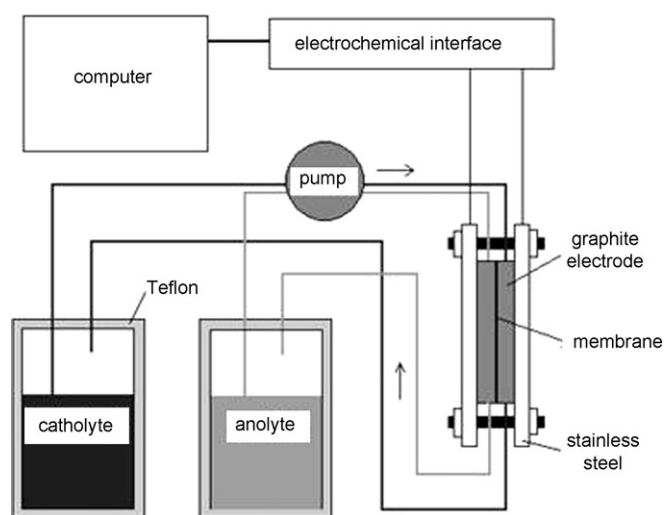

Fig. 1. Schematic illustration of the VRB setup in this work.

energy which is the product of C_{tc} and E^0 (standard cell potential, 1.246 V *vs.* SHE).

Open circuit voltage (OCV) was monitored at room temperature after the electrolytes were fully charged (charging at a constant voltage of 1.8 V, the full state-of-charge is defined as the state that the charging current is lower than 20 mA). The volume of the electrolytes was 40 mL. The cell life or essentially the membrane life was evaluated by immersing the membrane in 1 M VO_2^+ in 2 M H_2SO_4 solution for 15 days, and then test the changes in CE and EE of the cell with the immersed membrane.

3. Results and discussion

3.1. Physical–chemical properties of membranes

The physical–chemical properties of SPFEK membrane and Nafion 117 membrane are summarized in Table 1. Regarding that

Nafion membranes were well studied and the permeability of Nafion 117 membrane was relative low with contrast to other Nafion membranes, Nafion 117 membrane was chosen for easier comparison.

It can be seen from Table 1 that the water uptake as well as swelling ratio of SPFEK membrane is a bit higher than that of Nafion 117 membrane. Water uptake and swelling ratio are two important properties related to proton conductivity and dimensional stability of the membrane, so they should be neither too high nor too low to ensure good proton conductivity with appropriate dimensional stability. As presented in Table 1, The SPFEK membrane exhibited comparable proton conductivity to Nafion 117 membrane. High proton conductivity is crucially important to afford the high voltage efficiency of the battery.

In vanadium redox flow battery (VRB), the tensile strength of membranes is very important to assure its good mechanical stability when the electrolyte flow is passing through the membrane. As expected, SPFEK membrane showed a higher tensile strength than Nafion 117 membrane owing to its robust aromatic backbone. The elongation at break of Nafion 117 membrane was 223%, which is more than twenty times larger than that of SPFEK membrane.

3.2. Theoretic open circuit voltage of VRB

It has been reported that the standard open circuit voltage (OCV) of VRB single cell is 1.26 V [19], which was not in good accordance with the experimental data. The values from OCV curves are much larger than 1.26 V. By using Nernst equation, the following results can be drawn:

$$\varphi_+ = \varphi_+^0 - \frac{RT}{nF} \ln \frac{a_{[VO^{2+}]}}{a_{[VO_2^+]}} \tag{10}$$

$$\varphi_- = \varphi_-^0 - \frac{RT}{nF} \ln \frac{a_{[V^{3+}]}}{a_{[V^{2+}]}} \tag{11}$$

Table 1
Physical–chemical properties of SPFEK membrane and Nafion 117 membrane.

Membrane	IEC (mequiv. g^{-1})	Water uptake (%)	Swelling ratio (%)	Proton conductivity (s cm^{-1})	Tensile strength (Mpa)	Elongation at break (%)
Nafion117	0.91	20.5	10	3.48×10^{-2}	28	223
SPFEK	1.92	27.8	14	1.71×10^{-2}	38	11

$$E = \varphi_+ - \varphi_-$$
$$= \varphi_+^0 - \frac{RT}{nF} \ln\frac{a_{[VO^{2+}]}}{a_{[VO_2^+]}} - \varphi_-^0 + \frac{RT}{nF} \ln\frac{a_{[V^{3+}]}}{a_{[V^{2+}]}}$$
$$= E^0 - \frac{RT}{nF} \ln\frac{C_{[VO^{2+}]}C_{[V^{3+}]}}{C_{[VO_2^+]}C_{[V^{2+}]}} - \frac{RT}{nF} \ln\frac{\gamma_{[VO^{2+}]}\gamma_{[V^{3+}]}}{\gamma_{[VO_2^+]}\gamma_{[V^{2+}]}} \qquad (12)$$

where φ_+ and φ_- are the potentials of positive and negative half-cell, respectively. φ_+^0 and φ_-^0 are the corresponding standard half-cell potential. E is the cell potential. E^0 is the standard cell potential. R is the universal gas constant. T is the absolute temperature. a is the chemical activity for the relevant species. γ is the activity coefficient. F is the Faraday constant. n is the number of electrons transferred in the half-reaction.

For 1 M of VO^{2+} solution in sulfuric acid, the concentrations of VO^{2+} and VO_2^+ should fulfill the following equation (Eq. (14)) during charging and discharging processes:

$$y = 1 - x \qquad (13)$$

where x is the ion concentration of VO^{2+}, y represents the ion concentration of VO_2^+. Comparative to the ion pair of VO^{2+} and VO_2^+, the concentrations of V^{3+} and V^{2+} could apply for the same equation. Since the electrolytes are well circulated, we supposed that the activity coefficients are equal to 1. Additionally, $E^0 = 1.246$ V $vs.$ SHE, so Eq. (12) could be written in

$$E = 1.246 + \frac{RT}{nF} \ln\frac{(a-x)^2}{x^2} \qquad (14)$$

Fig. 2 shows the mathematic simulation curve of Eq. (14). As can be seen in the graph, the theoretic open circuit voltage depends on the state-of-charge of the electrolytes. The OCV of full-charged VRB ($x = 0$) is much higher than 1.26 V, which is in accordance with the experimental results.
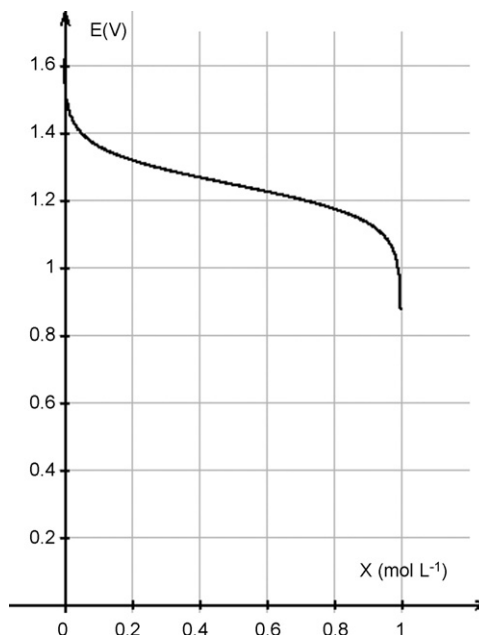

Fig. 2. Mathematic simulation curve of Eq. (14). E is the cell potential and x is the concentration of VO^{2+}.

3.3. Self-discharge characteristics of VRB

Self-discharge properties are very important in flow batteries because the electrolytes are easer to permeate through the separator from one half-cell to the other half-cell than any other solid batteries. Self-discharge is referred to the capacity loss of the
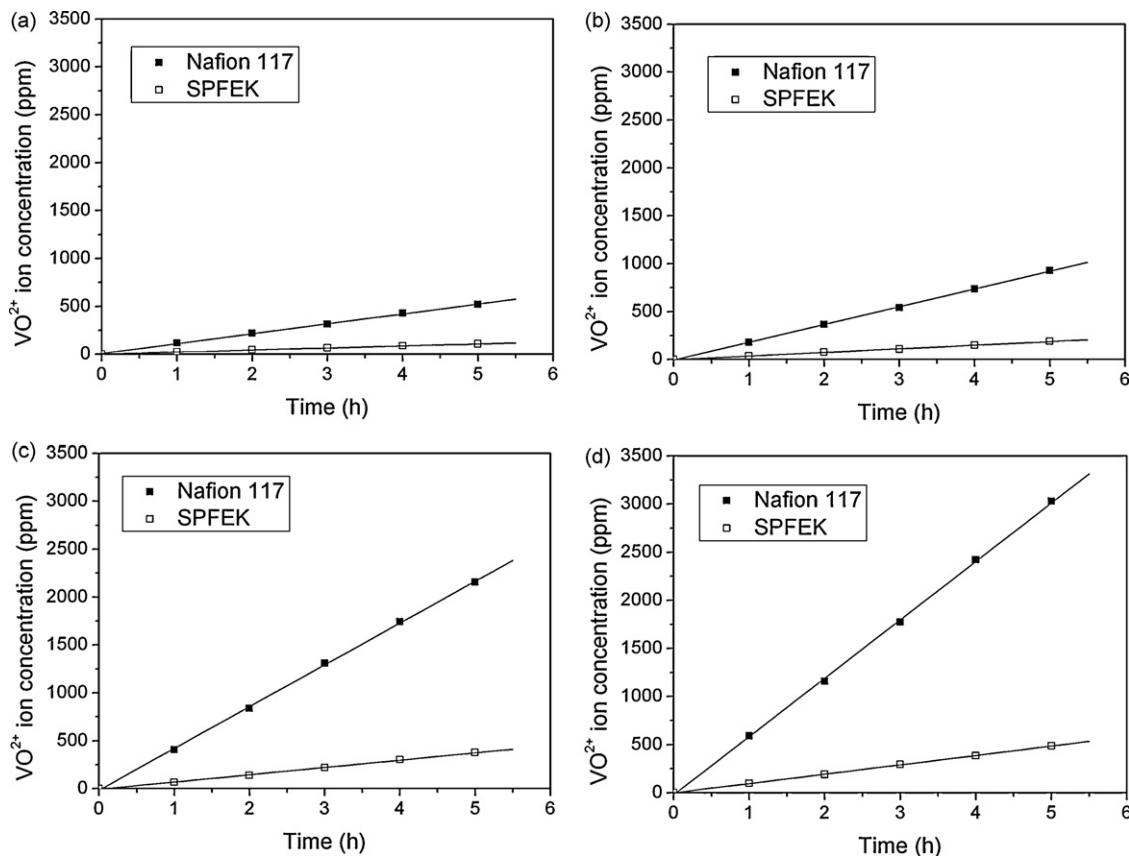

Fig. 3. The permeability of VO^{2+} $vs.$ time at the temperature of (a) 10 °C; (b) 25 °C; (c) 40 °C and (d) 50 °C.
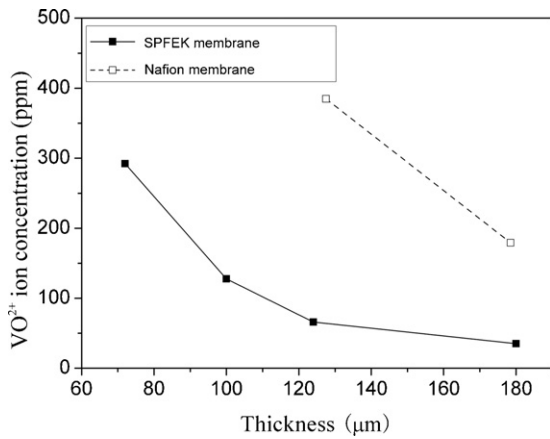
Fig. 4. Effect of the thickness of membranes on the permeability of VO^{2+} at room temperature.

Fig. 5. OCV of VRB assembled with SPFEK membrane and Nafion 117 membrane as a function of time.

battery without any connection between the electrodes. The self-discharge of VRB may be divided into capacity loss by permeation of vanadium ions and capacity loss by side reaction of electrolytes, such as reacting with air, electrode, membrane, impurities, and water and so on. The latter effect can be minimized and is beyond the discussion of this work.

The permeability of VO^{2+} through the membrane at 10 °C, 25 °C, 40 °C and 55 °C are shown in Fig. 3. The thickness of SPFEK membrane used is 180 μm, which is the same as that of Nafion 117 membrane. The vanadium ions permeability of the SPFEK membrane and Nafion 117 membrane was tested by monitoring the vanadium concentration in $MgSO_4$ solution at the same condition. It can be seen that the concentration of permeated VO^{2+} increase steadily with time as well as temperature. The permeability of vanadium ions across Nafion 117 membrane was higher than that of SPFEK membrane at same temperature.

The permeability of VO^{2+} vs. the thickness of membrane at a time interval of 1 h is shown in Fig. 4. As expected, the permeability of VO^{2+} decreases with the increase of the membrane thickness not only for SPFEK membranes but also for Nafion membranes. In addition, the vanadium permeability of Nafion membranes is higher than that of SPFEK membrane with the same thickness. In this paper, the SPFEK membrane with 99 μm in thickness was chosen for its appropriate permeability of vanadium ions. Nafion 117 membrane was chosen for comparison.

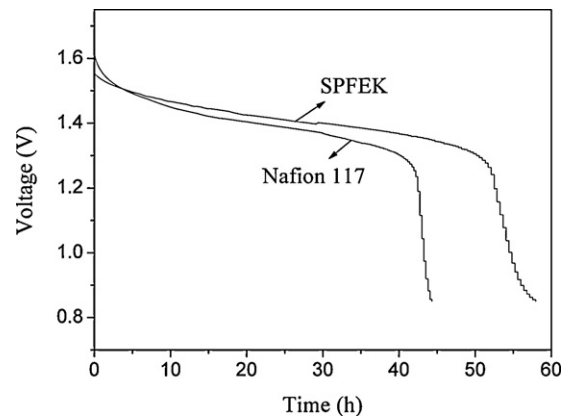The VO^{2+} diffusion coefficients (D) of membranes at room temperature were calculated by Fick's first law of diffusion on the assumption that a pseudo-steady-state condition inside the membrane.

$$J = -D\frac{\partial C}{\partial x} \tag{16}$$

The D of Nafion 117 membrane and SPFEK membrane were 24.89×10^{-7} cm^2 min^{-1} and 9.85×10^{-7} cm^2 min^{-1}, respectively. It can be concluded that SPFEK membrane has lower vanadium permeability than Nafion 117 membrane, which will be helpful to restrain the self-discharge of the VRB cell. The permeation of other states of vanadium ions was not evaluated for they are expected to behave in an analogous way.

Open circuit voltage (OCV) indicates the self-discharge of a VRB, which is resulted from the permeation of vanadium across the membrane and from the side reactions. The OCV curves with VRB single cell based on SPFEK and Nafion membranes are shown in Fig. 5. As can be seen, the curves decline slowly to 1.25 V firstly and then suddenly drop to 0.85 V. The time for OCV value maintaining above 1.25 V for the VRB assembled with SPFEK membrane is 52 h, which is 10 h longer than that of the VRB assembled with Nafion 117 membrane. The result was in good accordance with the permeation test, suggesting that SPFEK membrane would have a better performance than Nafion 117 membrane in VRB single cell test.

3.4. Performance of VRB single cell

The VRB single cell was fabricated by sandwiching the membranes in two pieces of graphite bipolar plates. The electrolytes were charged at a constant voltage of 1.8 V to full state-of-charge (when charging current is lower than 20 mA) and then discharged
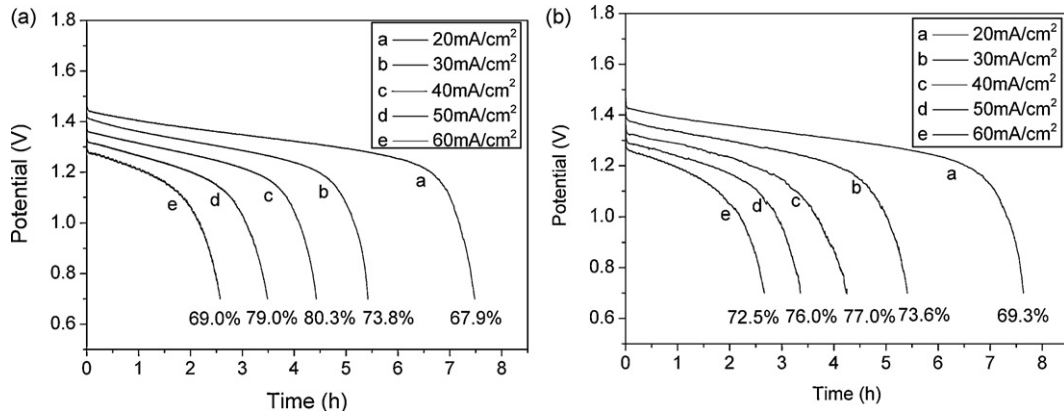

Fig. 6. Discharge characteristics of VRB (a) assembled with SPFEK membrane and (b) assembled with Nafion 117 membrane.

Table 2
CE and EE changes of VRBs assemble with the origin membrane and the membrane treated with VO_2^+ solution.

Membrane	Initial CE (%)	Final CE (%)	CE retention (%)	Initial EE (%)	Final EE (%)	EE retention (%)
Nafion 117	77.0	76.8	99.7	41.5	40.2	96.7
SPFEK	80.3	79.5	99.0	51.9	49.7	95.8

at different current densities and the voltage limit for discharge was controlled to 0.7 V. The discharge curves are shown in Fig. 6 with the coulombic efficiencies (CE) shown beneath each curve.

As shown in Fig. 6, the discharge behaviors of VRB assembled with SPFEK membrane are similar to that of VRB with Nafion 117 membrane. The voltage first dropped sharply from about 1.6 V to 1.28–1.45 V, and then it decreased to about 1.25 V slightly before it dramatically fell to the limit voltage. Higher discharge current densities give rise to higher polarization of the cell, resulting in lower conversion of chemical energy to electrical energy which is disadvantageous for the CE and EE. However, the amount of vanadium ions transported through the membrane will be reduced and the capacity loss by self-discharge will be diminished due to the shortened discharged time, which is beneficial for the CE and EE. Contrarily, lower current densities cause lower polarization of the cell but higher self-discharge. Therefore, the CE of VRB is determined by the synergetic effect of cell polarization and self-discharge at different discharge current densities. It is shown in Fig. 6 that the CE of VRB assembled with SPFEK membrane increase with the increasing of current density, reach a peak at 80.3% at 40 mA cm^{-2}, and then decrease as the current density keep raising. The CE of VRB assembled with Nafion 117 membrane has a similar trend, with its peak at 77% at 40 mA cm^{-2}.

The EE curves of VRB are presented in Fig. 7. It can be seen that the EE of VRB assembled with SPFEK membrane is generally higher than that of VRB with Naifon 117 membrane. This may be attributed to the larger self-discharge of the VRB with Nafion 117 membrane, which leads to longer time consumed for charging and shorter time holding for discharging. The EE of VRB assembled with SPFEK membrane peak at 51.9%, while the EE of VRB assembled with Naifon 117 membrane peak at 41.5%.

The CE and EE of the VRB in this paper are lower than those in other papers [9,19] because the testing conditions are different. However, it can be expected that higher concentration of the electrolytes will lead to higher CE and EE of the VRB.

Fig. 8 shows the polarization curves of VRB assembled with SPFEK membrane and Nafion 117 membrane. The voltage is determined as the average discharge voltage at the corresponding discharge current density. It can be seen that both the discharge
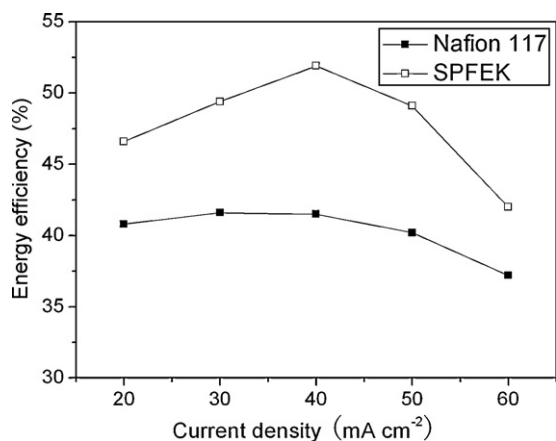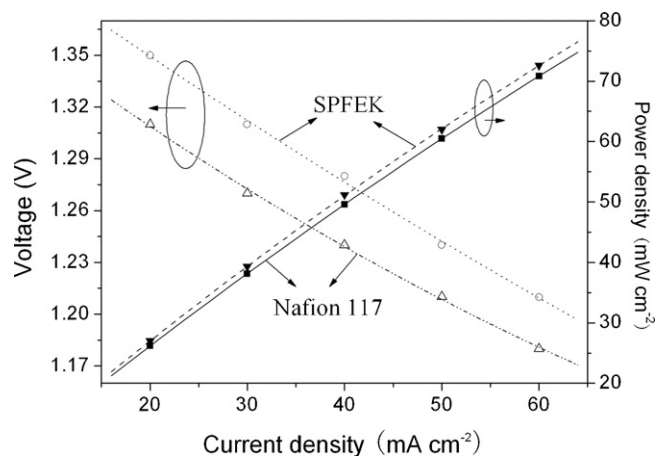

Fig. 8. Effect of discharge current density on average discharge voltage and power density of the VRB.

voltage and power density of VRB assembled with SPFEK membrane are higher than those of VRB assembled with Nafion 117 membrane. With the current density increasing from 20 mA cm^{-2} to 60 mA cm^{-2}, the power density increases from 27 mW cm^{-2} to 72.6 mW cm^{-2} for VRB assembled with SPFEK membrane.

3.5. Stability of membrane

The stability of membrane is one of the fundamental properties of VRB separator. Since the VO_2^+ was much more oxidative as compared to other vanadium ions, the membrane life was evaluated by immersing the membrane in 1 M VO_2^+ solution for 15 days at 25 °C to measure the changes in CE and EE. The discharge current density was set to 40 mA cm^{-2}. As shown in Table 2, there are not significant changes in CE and EE after the membrane being immersed. This indicates that both the SPFEK membrane and Nafion 117 membrane possess high stability in the electrolytes.

4. Conclusions

The as-made SPFEK membrane was investigated as the separator of VRBs and compared with Nafion 117 membrane. The SPFEK membrane displays lower vanadium ions permeability than Nafion 117 membrane with the same thickness. To compromise the resistance and vanadium permeability of the membrane, the thickness of SPFEK membrane was controlled to be 99 μm for the cell test. The self-discharge of VRB single cell was effectively restrained using the SPFEK membrane. As demonstrated in the discharge characteristics of VRB single cell, the energy efficiency and power density of VRB assembled with SPFEK membrane are generally higher than those of the VRB with Nafion 117 membrane. The highest coulombic efficiency (CE) of VRB with SPFEK membrane is 80.3% while the highest CE of VRB with Nafion 117 membrane is 77% at the same testing condition. From the membrane life test, it can be concluded that the SPFEK membrane is stable in the VO_2^+ electrolyte. Therefore, it appears to be a promising separator for vanadium redox flow battery application.

Fig. 7. Effect of discharge current density on energy efficiency (EE) of the VRB assembled with SPFEK and Nafion 117 membrane, respectively.

Acknowledgments

References

[1] M. Skyllas-Kazacos, M. Rychcik, R.G. Robins, A.G. Fane, M.A. Green, J. Electrochem. Soc. 133 (1986) 1057–1058.
[2] T. Sukkar, M. Skyllas-Kazacos, J. Appl. Electrochem. 34 (2004) 137–145.
[3] B. Tian, C.W. Yan, F.H. Wang, J. Appl. Electrochem. 34 (2004) 1205–1210.
[4] G.J. Hwang, H. Ohya, J. Membr. Sci. 120 (1996) 55–67.
[5] J.Y. Qiu, M.Y. Li, J.F. Ni, M.L. Zhai, J. Peng, L. Xu, H.H. Zhou, J.Q. Li, G.H. Wei, J. Membr. Sci. 297 (2007) 174–180.
[6] T. Mohammadi, M. Skyllas-Kazacos, J. Membr. Sci. 98 (1995) 77–87.
[7] Q.T. Luo, H.M. Zhang, J. Chen, P. Qian, Y.F. Zhai, J. Membr. Sci. 311 (2008) 98–103.
[8] T. Sukkar, M. Skyllas-Kazacos, J. Membr. Sci. 222 (2003) 249–264.
[9] J.Y. Xi, Z.H. Wu, X.P. Qiu, L.Q. Chen, J. Power Sources 166 (2007) 531–536.
[10] Y.L. Chen, Y.Z. Meng, A.S. Hay, Macromolecules 38 (2005) 3564–3566.
[11] S. Matsumura, A.R. Hill, C. Lepiller, J. Gaudet, D. Guay, Z.Q. Shi, S. Holdcroft, A.S. Hay, Macromolecules 41 (2008) 281–284.
[12] X.Y. Shang, S.H. Tian, L.H. Kong, Y.Z. Meng, J. Membr. Sci. 266 (2005) 94–101.
[13] K. Miyatake, Y. Chikashige, E. Higuchi, M. Wantanabe, J. Am. Chem. Soc. 129 (2007) 3879–3887.
[14] N. Asano, M. Aoki, S. Suzuki, K. Miyatake, H. Uchida, M. Watanabe, J. Am. Chem. Soc. 128 (2006) 1762–1769.
[15] M. Schuster, K.D. Kreuer, H.T. Andersen, J. Maier, Macromolecules 40 (2007) 598–607.
[16] B. Bae, K. Miyatake, M. Watanabe, J. Membr. Sci. 310 (2008) 110–118.
[17] Y.L. Chen, Y.Z. Meng, S.J. Wang, S.H. Tian, Y. Chen, A.S. Hay, J. Membr. Sci. 280 (2006) 433–441.
[18] E. Wiedemann, A. Heintz, R.N. Lichtenthaler, J. Membr. Sci. 141 (1998) 215–221.
[19] J.Y. Xi, Z.H. Wu, X.G. Teng, Y.T. Zhao, L.Q. Chen, X.P. Qiu, J. Mater. Chem. 18 (2008) 1232–1238.